Supporting information for

Photosensitizer-Conjugated Hyaluronic Acid-Shielded Polydopamine Nanoparticles for Targeted Photo-mediated Tumor Therapy

Jieun Han[‡], *Wooram Park*[‡], *Sin-jung Park, and Kun Na**

Center for Photomedicine, Department of Biotechnology, The Catholic University of Korea, 43 Jibongro, Wonmi-gu, Bucheon-si, Gyeonggi do, 14662, Republic of Korea

[‡]These authors contributed equally.

*Corresponding Authors

Kun Na, Ph.D.,

Center for Photomedicine, Department of Biotechnology

The Catholic University of Korea

43 Jibongro, Wonmi-gu, Bucheon-si, Gyeonggi do,

420-743, Korea

E-mail: kna6997@catholic.ac.kr

Experimental methods for supporting information

Biodegradation of PHPD-NPs: The PHPD-NPs (0.5 mg/mL) were suspended in PBS buffer (150 mM) solution. After treatment of hydroxyl peroxide (5 mM) for 24 h, the color change was observed and taken by digital camera.

Flow cytometry quantification of the CD44 receptor expression level: NIH3T3 and MDA-MB-231 cells were washed twice with DPBS and incubated with FITC labeled anti-CD44 antibody (clone IM7, LSBio, Seattle, Washington) at 4 °C for 30 min followed by washing with DPBS and subjecting to flow cytometry. The flow cytometry was performed using a BD FACS Canto II flow cytometry analyzer and FACS Diva software (BD Biosciences).

Energy-dependent endocytosis behavior of PHPD-NPs: MDA-MB-213 cells were incubated with PHPD-NPs (0.1 mg/mL) in a SF culture medium for 4 h at 4 °C or 37 °C under 5 % CO_2. After incubation, the cells were analyzed by flow cytometry and CLSM imaging system.

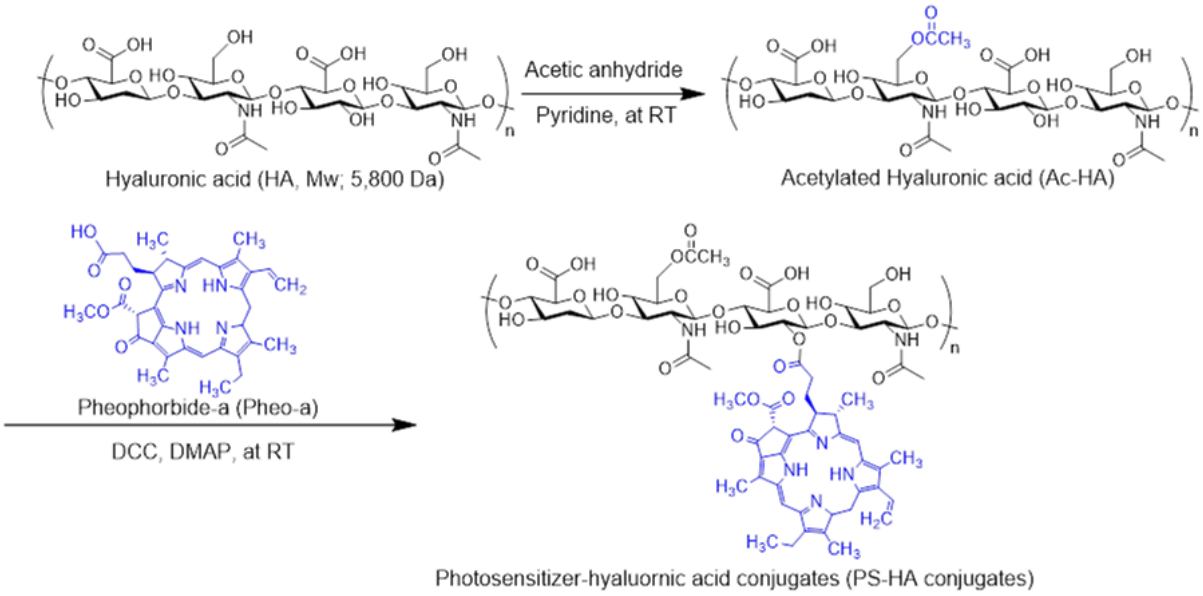

Figure S1. Chemical synthetic route for PS-HA conjugates.

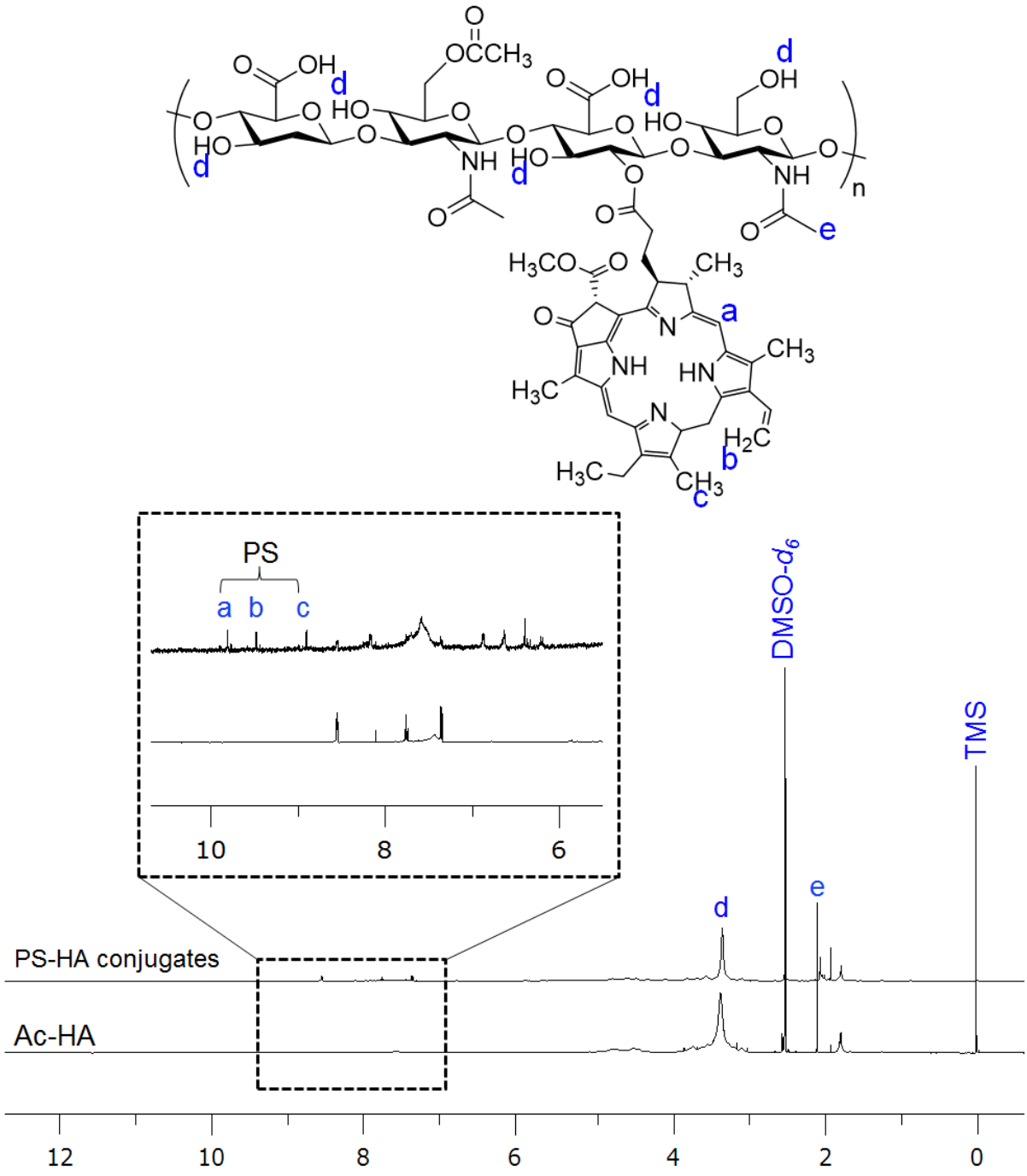

Figure S2. ^{1}H-NMR analysis of Ac-HA and PS-HA conjugates in DMSO-d_6.

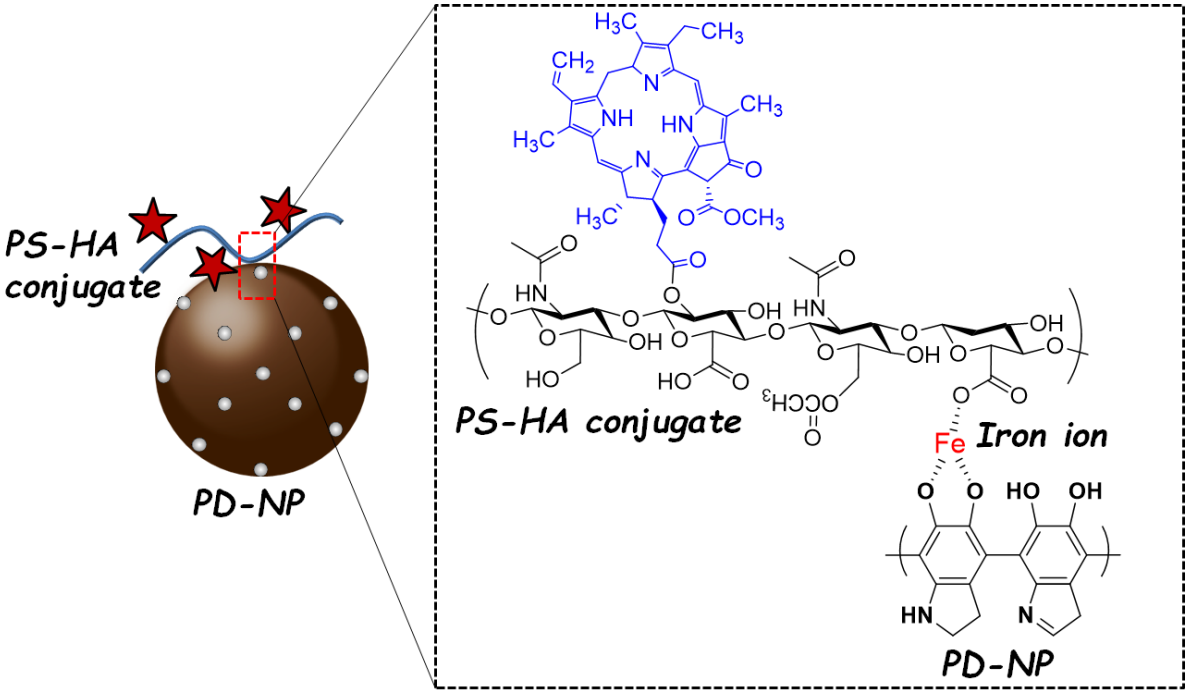

Figure S3. Schematic illustration of iron-mediated coordination in preparation of PHPD-NPs.

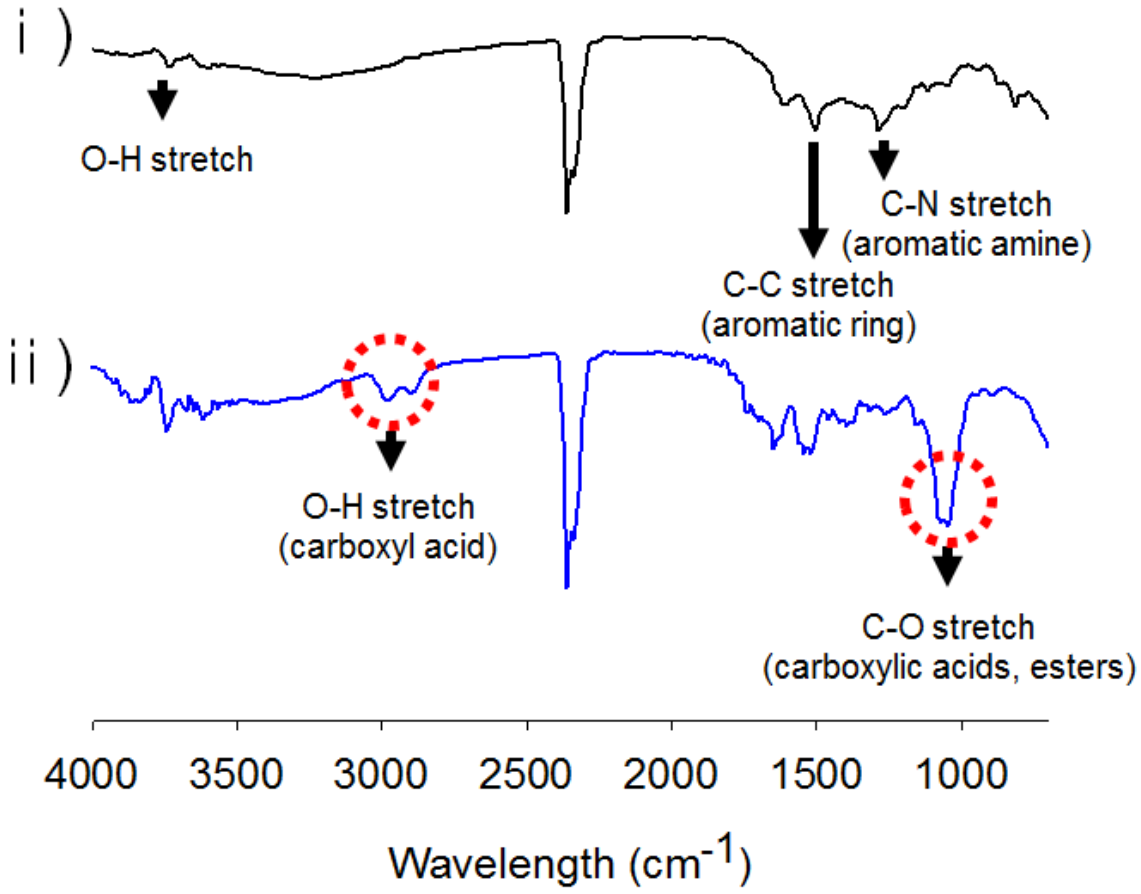

Figure S4. FT-IR analysis of ⅰ) PD-NPs and ⅱ) PHPD-NPs.

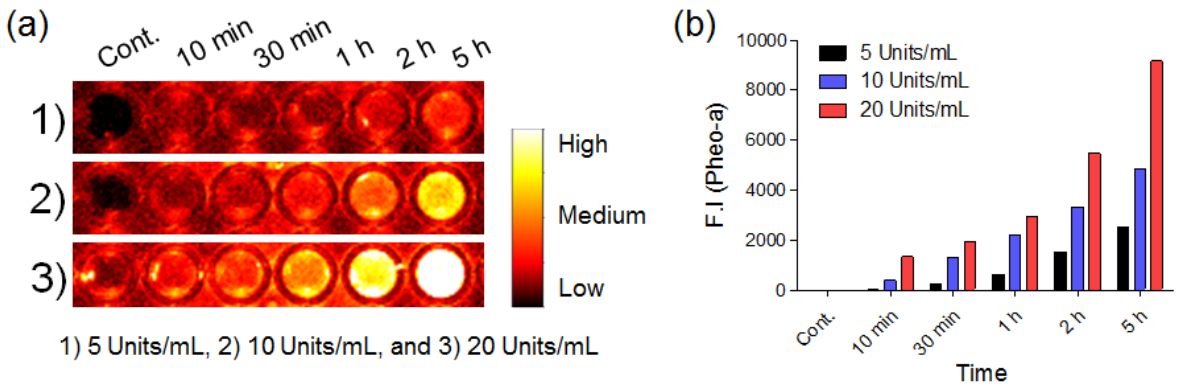

Figure S5. Photo-activity measurement of PHPD-NPs in the present of HAase. (a) Fluorescent images and (b) quantitative fluorescent intensity analysis of the PHPD-NPs incubated with different concentration of HAase over time.

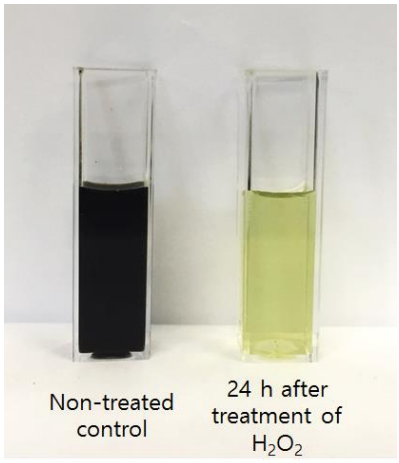

Figure S6. Biodegradation of PHPD-NPs. Photograph of non-treated PHPD-NPs dispersion (0.5 mg/mL) and after addition of H_2O_2 (5 mM). The color (dark brown) of PHPD-NPs faded after treatment of H_2O_2.

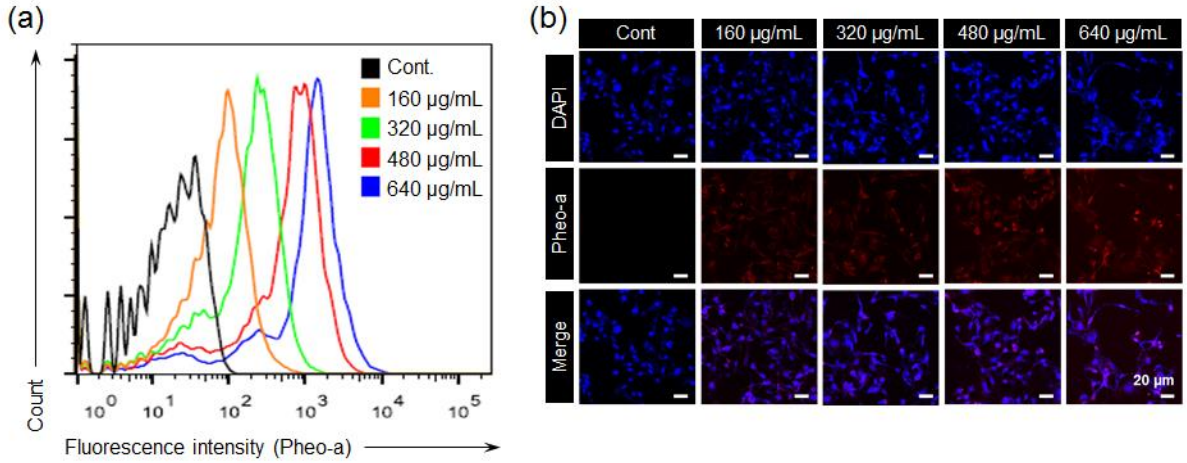

Figure S7. *In vitro* cellular internalization of PHPD-NPs at different concentrations of PD-NPs: (a) Flow cytometry quantification of the cellular internalization of PHPD-NPs against MDA-MB-231 cells at different concentrations of PD-NPs. (b) Confocal laser scanning microscopy image of MDA-MB-231 cells treated with PHPD-NPs as different concentration. (Incubation time: 4 h, scale bar: 20 μm).

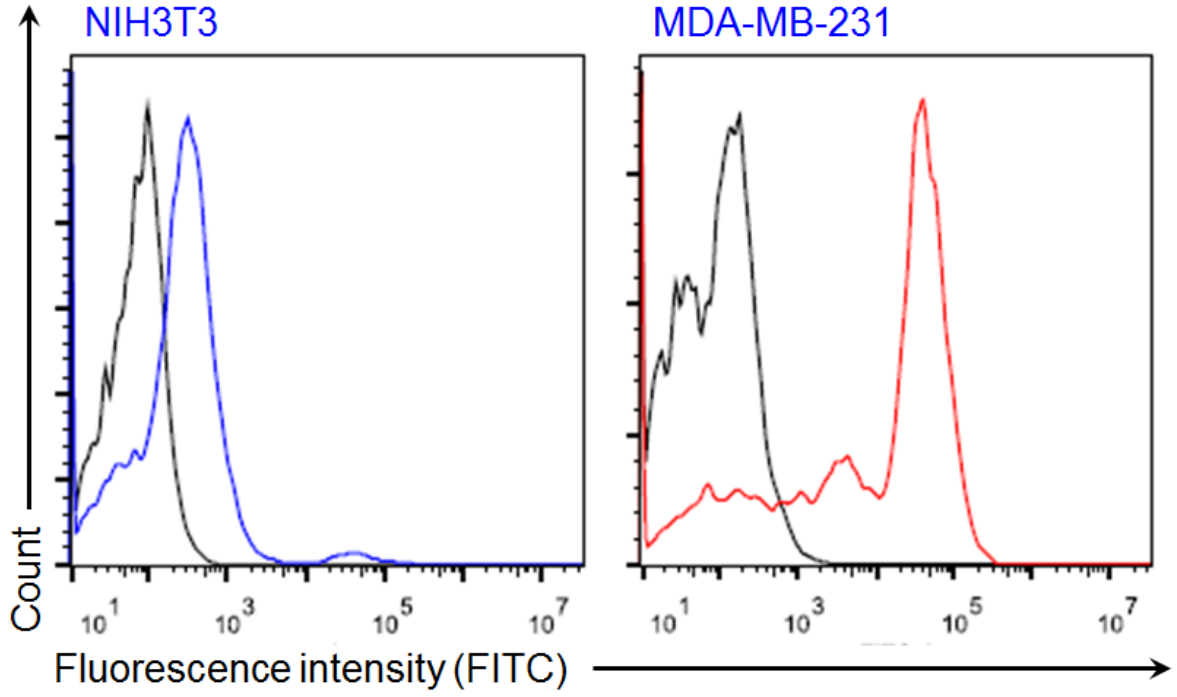

Figure S8. Flow cytometry quantification of the CD44 receptor expression level in NIH3T3 and MDA-MB-231 cells.

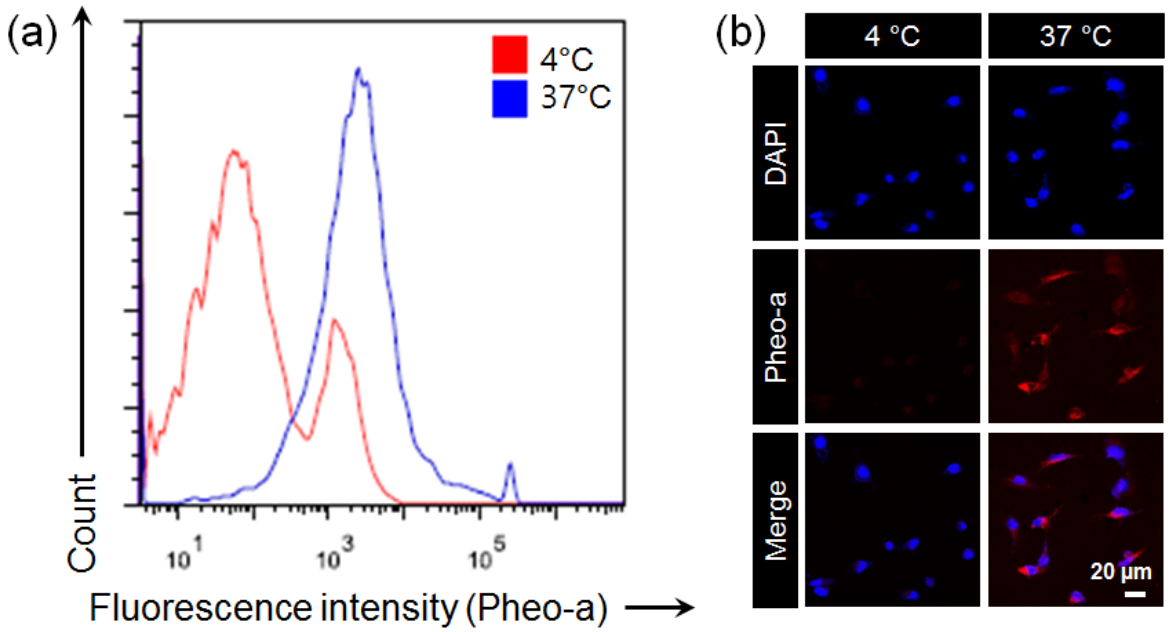

Figure S9. Energy-dependent endocytosis behavior of PHPD-NPs. (a) Flow cytometry quantification of the cellular internalization of PHPD-NPs against MDA-MB-231 cells at different temperatures (4 and 37 °C). (b) Confocal laser scanning microscopy images of MDA-MB-231 cells treated with PHPD-NPs at different temperatures (4 and 37 °C).

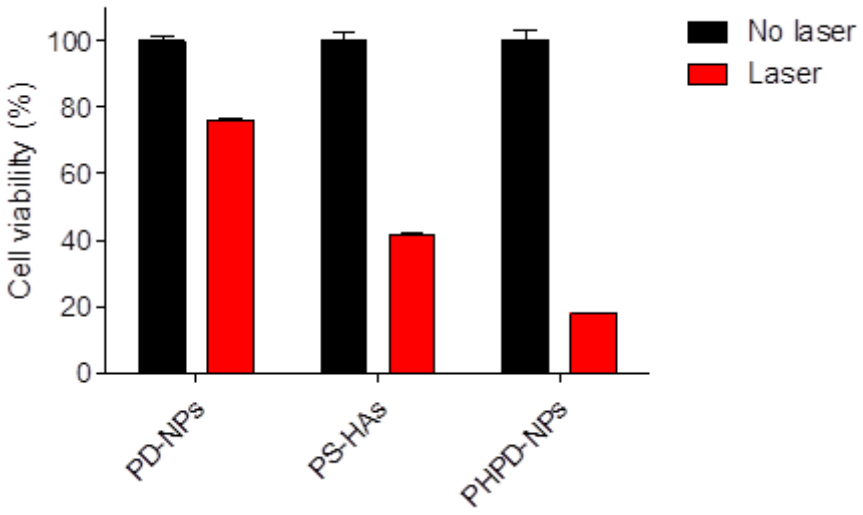

Figure S10. Cell viability of MDA-MB-231 cells treated with PD-NPs, PS-HAs and PHPD-NPs under laser irradiation at 3.0 J/cm^2 power.

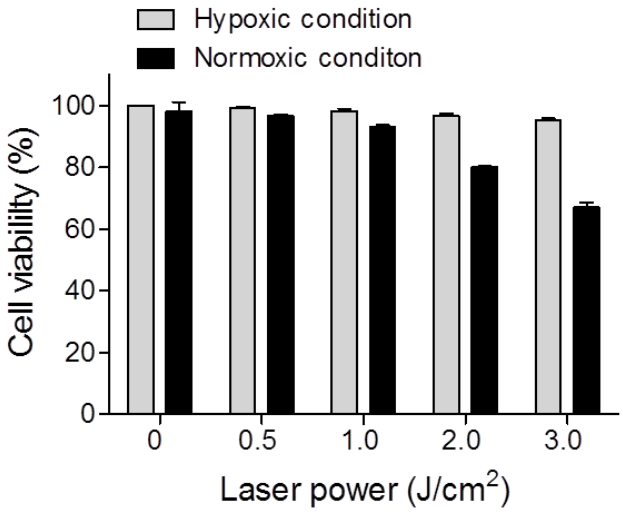

Figure S11. Cell viability of MDA-MB-231 cells treated with free pheo-a (2.4 μg/mL) in the hypoxic and normoxic conditions under different laser irradiation power. The photo-mediated cytotoxicity of free pheo-a was significantly decreased in hypoxic conditions when compared with that of normoxic conditions.

Table S1. Chemical characterization of PS-HA conjugates

Code	DS of acetyl groups[(a)]	DS of PS molecules[(b)]
PS-HA	0.40 ±0.02	0.10 ±0.03

[(a)]Degree of substitution of acetyl groups per HA unit (2 glucose rings), determined by ^{1}H-NMR (n=3).
[(b)]Degree of substitution of pheo-a molecules per HA unit (2 glucose rings), determined by UV-Vis spectrophotometer (n=3).